TENSILE LAP SPLICES

PART I: RETAINING WALL TYPE, VARYING MOMENT ZONE

by

Phil M. Ferguson

and

Eduardo A. Briceno

Research Report No. 113-2

Research Project Number 3-5-68-113
Splices and Anchorage of Reinforcing Bars

P R E F A C E

This Part 1 (Research Report 113-2) is a progress report on one phase of the general project "Splices and Anchorage of Reinforcing Bars." It covers an investigation of #11 bar splices (a few #8) under a condition which models the necessary splices at the base of the stem of a cantilever retaining wall. While an extension of the present work will continue into 1969-1970, the present findings call for quite substantial changes from the present AASHO specifications for such splices. From the standpoint of safety it is not desirable to withhold the present findings for these later tests.

This Part 1 of the overall report on "Tensile Lap Splices" will be followed by further parts:

Part 2: Splices of #14 and #18 Bars (early 1970)

Part 3: The continuation of Part 1 with checks on proposed theory, either as a follow-up report or as a report replacing Part 1 (1971)

Research Report 113-1, entitled "Test of Upper Anchorage of No. 14S Column Bars in Pylon Design" by K. S. Rajagopalan and Phil M. Ferguson published August 1968, covers another phase.

The opinions, findings, and conclusions expressed in this publication are those of the authors and not necessarily those of the Bureau of Public Roads.

Eduardo A. Briceno

Phil M. Ferguson

July 1969

S U M M A R Y

An investigation of the strength of closely spaced lap splices in retaining wall stems is reported. Splitting type failures typically occurred, often stripping the entire cover off of the splices. This study of 32 specimens with #11 and #8 bars is continuing into 1969-1970.

It is concluded in Part A that the 1965 AASHO specification for splices does not provide a safe guide unless it is seriously modified. The necessary immediate modifications are developed for the case of 2 in. clear cover, with a splice length increasing as lateral spacing decreases and the present specification adequate only for unusually wide spacings.

In Part B a tentative theoretical treatment of lap splice length based on the several observed types of splitting failure is presented. Although this theory is potentially a considerable advance over present knowledge, certain transition stages and limits must be better defined before it can be used with confidence. A portion of the 1969-1970 program is directed to this end.

IMPLEMENTATION OF RESEARCH RESULTS INTO
TEXAS HIGHWAY DEPARTMENT OPERATION

It is recommended that the design of lap splices in the stem of retaining walls be increased from the present AASHO requirement of 19D (D is bar diameter) for f_y = 40 ksi and f'_c = 3500 psi to the following lap length which is a function of the lateral spacing S and D:

$$L_s = 19D \div (0.13\ S/D - 0.04) \geqslant 19D$$

This requires the following lap lengths:

S/D = 3	S = 4.2"	L_s = 54D
4	5.6"	40D
5	7.0"	31D
6	8.5"	26D
8 or more	11.2"	19D

These lengths apply where all bars are spliced at the point of maximum moment and assume at least a 2 in. clear cover provided.

Where splices are staggered in location such that not more than half are spliced at one wall level, their lengths can be reduced to 0.8 the above. However, this is not documented well enough to justify anywhere less than a 19D lap.

For higher strength reinforcing bars the splice length L_s should be increased by the factor $f_y/40$ (with f_y expressed in ksi). For concrete strengths <u>less</u> than 3500 psi the value of L_s should be increased by the factor $3500/f'_c$. The two factors could be cumulative.

For clear cover <u>less</u> than 2 in. the laps tabulated above for the larger spacings are probably not adequate, but this investigation has not adequately explored thinner covers. Figure 12 estimates, on very skimpy information, that one bar diameter of clear cover (C/D = 1) might require a 36D splice lap even if the spacing were wide, and the tabulated longer lap at S/D of 3 or 4.

These recommendations do not apply to splices in a constant moment length which should be 15 to 25 percent longer, the exact value not yet closely defined in terms of spacing.

INTRODUCTION

Existing Splice Requirements

For a tension splice in a reinforced concrete member, a lap splice (Fig. 1a) is required unless welding or a mechanical splice is used. Both the 1965 AASHO specification and the 1963 ACI Building Code use a reduced value of bond stress for a splice, but the net design requirements differ substantially.

The AASHO specification requires a WSD splice length L_s which is 4/3 as long as required for a uniform bond stress of $0.10 \, f'_c$ (with a maximum of 350 psi). Since for intermediate grade bars the working value of $f_s = f_y/2$, this leads at ultimate to:

$$2 \, \Sigma_o \, u \, L_s = A_s f_y \qquad \text{or} \qquad 2\pi D(0.10 f'_c) 0.75 L_s = \pi D^2 f_y / 4$$

$$L_s = f_y D / (0.60 f'_c)$$

For f_y = 40 ksi and f'_c = 3500 psi, L_s = 19D = 26.8" for #11
                                                      = 19" for #8

For f_y = 60 ksi and f'_c = 3500 psi, L_s = 28.5D = 40.2" for #11
                                                        = 28.5" for #8

The ACI Building Code (318-63) has the same general requirement, 4/3 the development length, for widely spaced splices but the basic USD bond stress permitted is $9.5 \sqrt{f'_c}/D$, thus varying with the bar size. For closely spaced splices the required length is further increased by 20 percent. For f_y = 40 ksi, f'_c = 3500 psi, and closely spaced splices:

$$\pi D(9.5 \sqrt{f'_c}/D) L_s (0.75/1.20) = \pi D^2 f_y / 4$$

$$L_s = f_y D^2 / (23.7 \sqrt{f'_e})$$

$$= 28.5 D^2 \text{ or } 40.2D = 57" \text{ for #11}$$

$$28.5D = 29" \text{ for #8}$$

For f_y = 60 ksi, all lengths increase in the ratio 60/40:

$$60.3D = 85" \text{ for } \#11$$
$$42.7D = 43" \text{ for } \#8$$

These lengths are greatly in excess of the AASHO requirements, especially for the #11 bars.

Top cast bars under both specifications call for lower bond stresses and longer splices.

The Splitting Problem

For bond on deformed bars in general, and for tension splices in particular, the most common failure is by splitting of the concrete parallel to the bar axis. The bearing forces on the bar lugs, instead of being parallel to the axis of the bar, have a radial component which reacts on the surrounding concrete, like water pressure in a pipe, to cause failure by splitting on the weakest plane.

In the stem of a cantilever retaining wall the closely spaced splices accumulate these splitting forces with resulting weakness in the plane of the vertical bars.

Project Objective

The primary objective of this Part I of the investigation was to study the behavior of the retaining wall type of splice and to formulate modified design requirements if found desirable.

This report itself is presented in two parts. Part B is a tentative theoretical analysis which is still under evaluation.

P A R T   A

RETAINING WALL SPLICES

Scope of Investigation

Thirty-two beams were tested, 27 having #11 bar splices, 4 having #8 bar splices, and 1 having #9 main bars spliced to #11 dowel bars. The percentage of longitudinal steel was generally 1.67 percent of A432 steel, the beam size being varied when bar diameter or spacing was changed. Concrete strength was typically from 3000 to 4000 psi.

Various lateral spacings of splices and various arrangements of the spliced bars were used. Typically two splices were used in a test member, but some specimens had 3 or 4 splices and some splices were staggered. Five beams used the equivalent of ties or stirrups over the splices.

Test Specimens

The shape of a retaining wall section (Fig. 1b) is not convenient for testing purposes. The wall stem was simulated by a beam length of constant cross section. The base of the wall was replaced (Fig. 1c) by a perpendicular (stub) section projecting from both the tension and compression faces of the beam, and the beam itself was extended with a dummy or loading section. The beam load was applied through the stub section in a manner crudely simulating the flexural compression from the toe of the retaining wall (Fig. 1d). Although the test specimen is greatly different from the wall, its behavior around the splice was planned to be similar to that of the wall.

The loading of the member was also simplified, such that a constant shear and linear moment distribution existed over the splice rather than the more complex soil pressure loading assumed on a wall.

The various specimen details are shown in Fig. 2 as cross sections and in tabular form in Table 1. The table also shows by sketches the arrangement of bars at the laps.
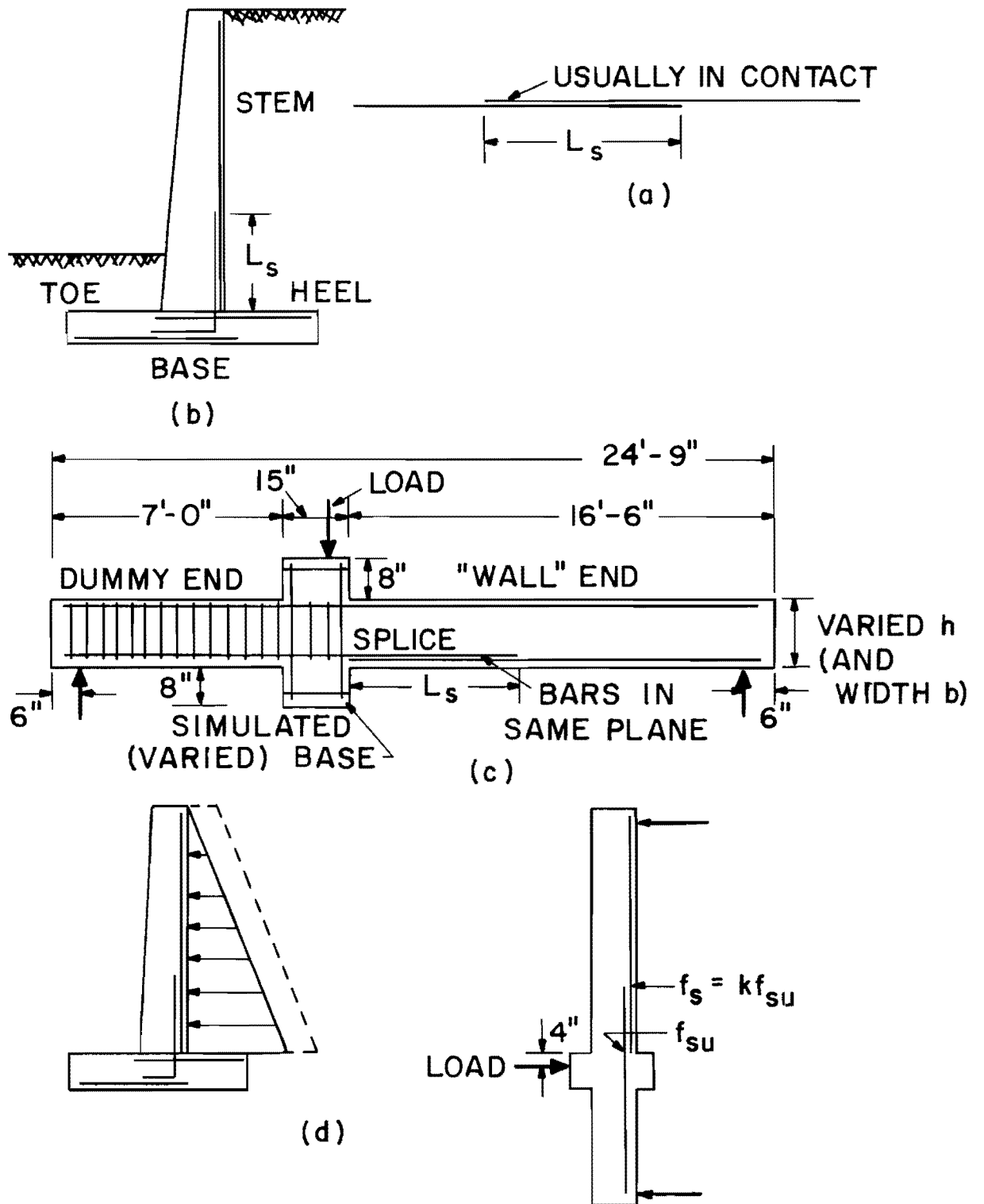
FIG. I. TEST CONCEPT. (a) BASIC LAP SPLICE. (b) CANTILEVER RETAINING WALL WITH TYPICAL STEM BAR SPLICES. (c) TEST SPECIMEN TO SIMULATE WALL SPLICE. (d) WALL LOADING COMPARED TO TEST LOADING.
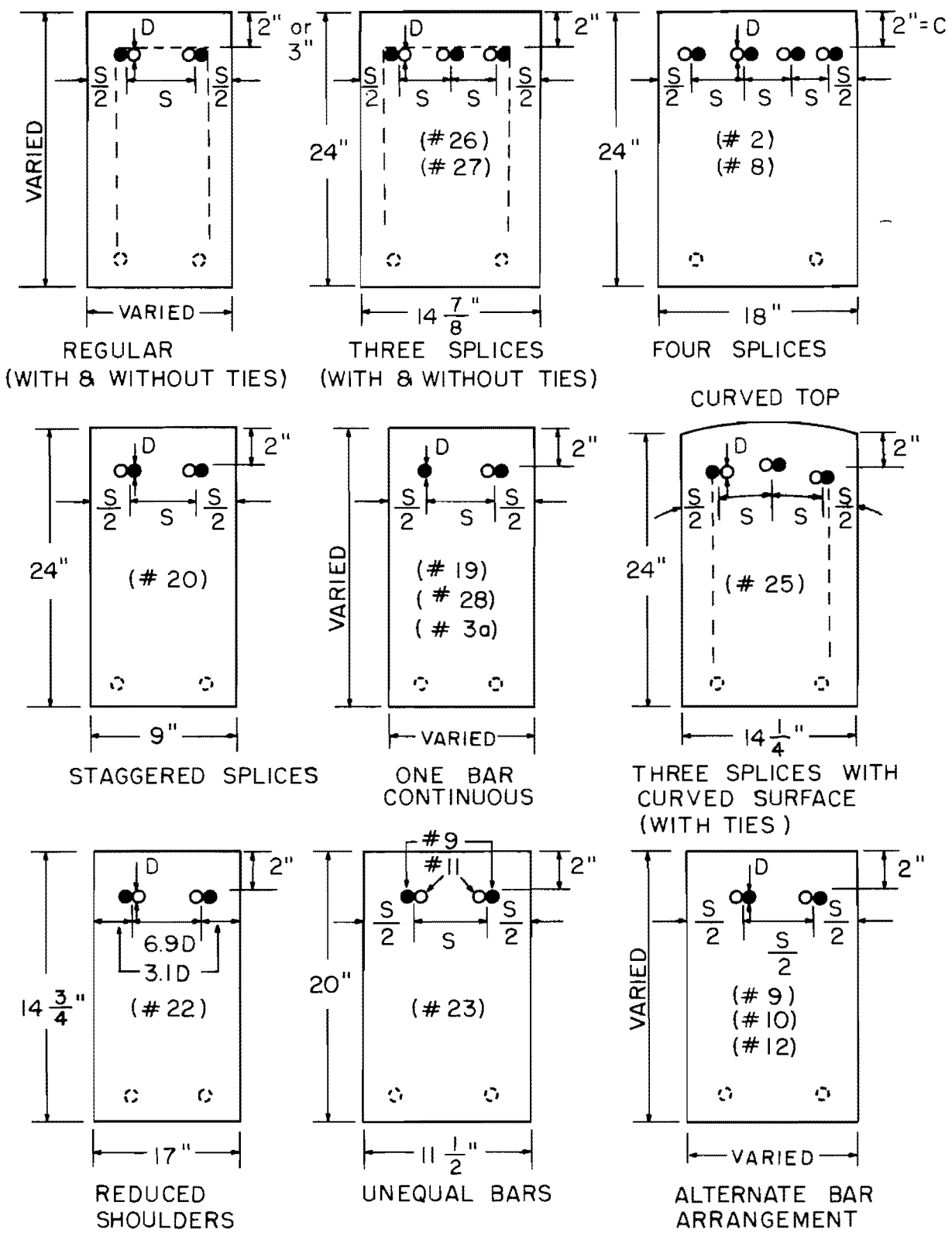
FIG. 2. GEOMETRICAL ARRANGEMENT OF VARIABLES IN TEST SPECIMENS. THE DOWEL BARS INTO THE "BASE" ARE UNSHADED.

TABLE 1. DETAILS OF SPECIMENS
Clear cover is 2", except 3" for beam 16.
f_y = 65 ksi for beams 1-25, incl.; 70 ksi for 26, 27, 28, and 1a-4a, incl.

Beam No.	Width b in.	Total h in.	Bar Diam in.	Spcg. in Bar Diam.	Splice L_s in.	Split Cyl. f_t' psi	f_c' psi	Stirrup or U-ties	Bar Arrangement
1	9.06	24.06	1.41	3.2	85.0	298	2800	None	
2	18.06	23.94	1.41	3.2	85.0	455	3970	"	
3	14.25	17.00	1.41	5.0	85.0	441	3750	"	
4	22.69	12.19	1.41	8.0	65.5	470	3680	"	
5	9.00	24.13	1.41	3.2	85.0	420	3900	"	
6	22.57	12.13	1.41	8.0	49.5	415	3570	"	
7	9.31	24.06	1.41	3.3	57.5	370	2920	"	
8	18.31	24.00	1.41	3.2	85.0	---	3360	"	
9	9.03	24.00	1.41	3.2	85.0	372	3060	"	
10	14.36	17.00	1.41	5.1	85.0	282	2450	"	
11	9.19	24.06	1.41	3.3	85.0	310	3200	"	
12	11.68	20.00	1.41	4.1	65.0	435	4250	"	
13	14.31	17.00	1.41	5.1	44.0	380	3380	"	
14	17.00	14.89	1.41	6.0	33.0	334	3050	"	
15	14.13	17.00	1.41	5.0	65.0	372	3340	"	
16	14.13	17.06	1.41	5.0	44.0	354	3060	"	
17	17.06	14.75	1.41	6.0	50.0	351	3550	"	
18	9.00	24.00	1.41	3.2	85.0	400	4270	10-#3@9"	
19	9.15	24.00	1.41	3.2	57.5	427	3720	None	
20	9.12	24.13	1.41	3.2	57.5	374	3250	"	
21	9.00	24.00	1.41	3.2	85.0	390	4190	4-#2@5.2"	
22	17.06	14.87	1.41	6.9*	50.0	356	3900	None	
23	12.00	20.00	1.41} 1.13}	4.3	65.0	360	3600	"	#9
24	9.25	24.00	1.41	3.3	57.5	392	3610	8-#2@7.4"	
25	14.25	24.00	1.41	3.4	42.3	340	3340	8-#3@6"	
26	15.00	24.00	1.41	3.5	42.3	361	3200	8-#3@6"	
27	15.13	24.13	1.41	3.6	42.3	360	3270	None	
28	14.13	17.00	1.41	5.0	44.0	371	3290	"	
1a	8.00	15.75	1.00	4.0	47.0	---	2770	"	
2a	10.00	13.00	1.00	5.0	32.0	402	3920	"	
3a	6.50	20.00	1.00	3.2	42.0	370	3750	"	
4a	6.25	20.00	1.00	3.1	42.0	475	4350	"	

*This is center spacing; edge distances smaller, to give 6.0D average.

Preparation and Testing

Specimens were cast on their side from a ready mixed concrete made with high early strength cement (Type III) and Colorado River sand and gravel (1.5 in. maximum). The water-cement ratio was 6.6 gallons per sack, cement factor 4.5 sacks per cubic yard, and slump 2 in. to 3 in.

The spliced bars were A432 grade deformed bars with stress-strain curves shown in Fig. A1 in Appendix. Ties were of intermediate grade with f_y = 56.5 ksi for #3 bars and f_y = 49 ksi for the plain #2 bars.

Resistance strain gages were mounted on the surface of the spliced bars at approximately the quarter points and at the loaded ends, sometimes on one splice, sometimes in all splices. The bar size was such that these gave a minimum interference with bond.

The specimens were tested on their side, supported on 7 in. diameter rollers, and loaded by a hydraulic jack against steel yoke reaction. The reaction at the end containing the splice was monitored by a load cell. Incremental loading was applied up to failure.

The ultimate steel stress f_{su}, the ratio $k = f_s/f_{su}$ (both based on strain readings), and type of failure are tabulated in Table 2, along with other calculations discussed later.

Splice Behavior

The member first cracked in flexure at the higher stressed end of the splice, adjacent to the loading stub. The tendency toward the formation of diagonal cracks near the loading stub was not significant with this size of specimen, contrary to some earlier findings with shallow members. Flexural cracking progressed along the splice as loads were increased, with the crack at the outer end of the splice appearing somewhat ahead of neighboring flexural cracks. There was a considerable tendency for a premature diagonal crack to start from this end of the splice unless a few stirrups were present there.

Splitting along the bars developed with increasing load, only on the sides of the beam for closely spaced splices, but for wider spacings first on the tension face followed by side splitting before failure. Four types of failure were observed, as noted in the last column of Table 2.

TABLE 2. TEST DATA AND CALCULATIONS

Beam No.	f_{su} psi	f'_c psi	L_s/D	Spcg. in bar diam. c-c	$k = f_s/f_{su}$	Cover C/D	Split cyl.f'_t psi	Calc. f'_t psi	f'_t ratio (calc)/(cyl)	u_{test} psi	$\frac{0.5\ u}{u_{AASHO}}$	Type of Failure
1	46.0	2800	60.3	3.2	0.78	1.41	298	279	0.94	191	0.45	Side split
2	76.0	3970	60.3	3.2	0.56	1.41	455	408	Flex.	315	0.60	Flexure
3	73.7	3750	60.3	5.0	0.54	1.41	441	254	Flex.	306	0.58	Flexure
4	73.7	3680	46.4	8.0	0.61	1.41	470	170	Flex.	397	0.76	Flexure
5	60.5	3900	60.3	3.2	0.71	1.41	420	359	0.85	251	0.48	Side split
6	71.5	3570	35.1	8.0	0.76	1.41	415	238	Flex.	509	0.97	Flexure
7	44.7	2920	40.8	3.3	0.74	1.41	370	367	1.08	274	0.63	Side split
8	69.4	3360	60.3	3.2	0.55	1.41	---	358	---	288	0.57	Diag. Tens.
9	59.0	3060	60.3	3.2	0.72	1.41	372	349	0.94	245	0.53	Diag. Tens. (Near split)
10	73.7	2450	60.3	5.1	0.55	1.41	282	255	Flex.	306	0.83	Flexure
11	59.4	3200	60.3	3.3	0.80	1.41	310	353	1.13	246	0.51	Diag. Tens. (Near split)
12	71.3	4250	46.1	4.1	0.66	1.41	435	506	1.16	387	0.74	Face-side split
13	56.0	3380	31.2	5.1	0.88	1.41	380	439	1.15	449	0.88	Face-side split
14	41.0	3050	23.4	6.0	0.97	1.41	334	337	1.01	438	0.96	Face-side split
15	72.0	3340	46.1	5.0	0.68	1.41	372	349	0.94	390	0.78	Face-side split
16	55.0	3060	31.2	5.0	0.78	2.13	354	415	1.17	441	0.96	Face-side split
17	59.5	3550	35.5	6.0	0.81	1.41	351	306	0.87	419	0.80	Face-side split
18	75.0	4270	60.3	3.2	0.55	1.41	400	406	1.01	311	0.58	Flexure
19	59.5	3720	40.8	3.2	0.74	1.41	427	471	1.10	365	0.69	Side split
20	56.0	3250	40.8	3.2	0.65	1.41	374	385	1.01	343	0.70	Side split
21	64.0	4190	60.2	3.2	0.64	1.41	390	366	0.94	265	0.51	Side split
22	77.0	3900	35.5	6.9*	0.70	1.41	356	313	0.88	543	1.04	Face-side split
23	56.0	3600	46.1	4.3	0.80	1.41	360	421	1.17	304	0.58	Face-side split
24	65.0	3610	40.8	3.3	0.75	1.41	392	545	1.39	398	0.76	Side split
25	63.7	3340	30.0	3.4	0.87	1.41	340	545	1.60	531	1.06	Side split
26	58.0	3200	30.0	3.5	0.79	1.41	361	559	1.55	483	1.00	Side split
27	40.0	3270	30.0	3.6	0.91	1.41	360	405	1.12	333	0.68	Side split
28	60.0	3290	31.2	5.0	0.87	1.41	371	451	1.20	481	0.98	Face-side split
1a	51.0	2770	47.0	4.0	0.75	2.00	---	240	----	271	0.66	Side split
2a	59.0	3920	32.0	5.0	0.91	2.00	402	463	1.14	461	0.80	Face-side split
3a	63.5	3750	42.0	3.2	0.74	2.00	370	380	1.03	378	0.72	Side split
4a	59.5	4350	42.0	3.1	0.72	2.00	475	551	1.15	354	0.67	Side split

*This is center spacing; edge distance smaller, to give 6.0D average.

1. Flexure, by yielding of the steel and secondary failure in compression.

2. Diagonal tension, starting from the lower stressed end of the splice.

3. Side split failure, that is, bond splitting all across the plane of the bars, with little or no splitting on the tension face, as in Fig. 3.

4. Face-and-side split failure, that is, splitting first on tension face and then all across the plane of the bars.

Flexural failure implies a splice entirely adequate for the beam in which it was used. The lowest steel stress at such a failure was 71.5 ksi.

Only three beams failed in diagonal tension. Each was premature failure (in terms of the ACI USD allowable v_c of $2 \sqrt{f_c'}$) but two were in such a stage of splitting as to be judged as near splitting failure. The data for all three plot very close to those of the splitting failures and no distinction has been maintained between the two types of failure.

It appeared obvious from the splitting behavior that a third kind of splitting failure might be possible when either a wide splice spacing or a thin face cover was used. This failure would start as a normal face split followed by two flatly inclined face splits which would open up a symmetrical, flat V-groove over the splice. No such failure occurred in this series, but a single picture of this type was found in the files from earlier splice tests.

Splitting failures, except with stirrups, were sudden and sharply defined, leaving a wide crack at the failure surface (Fig. 3).

General Influence of Splice Spacing

A casual inspection of the splitting failure data indicates that the computed average bond stress over the splice length was considerably influenced by the lateral spacing of splices. When the ratio of half the average ultimate bond stress relative to the AASHO allowable (WSD) bond stress is plotted in Fig. 4, omitting special cases discussed later, all ratios are extremely low. In

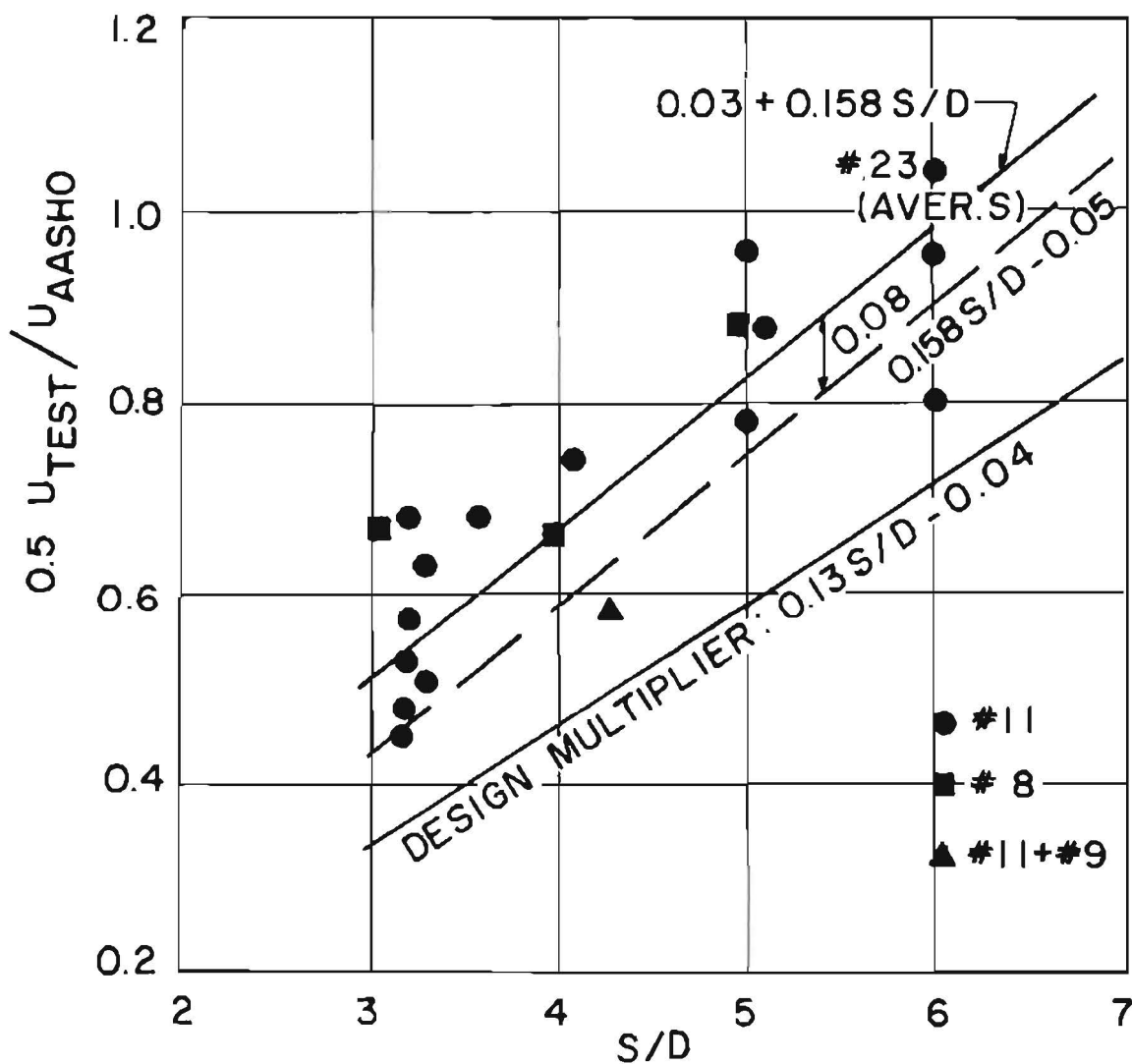FIG.3. SIDE SPLIT FAILURE OF BEAM NO.5

FIG.4. BOND EFFICIENCY IN TERMS OF
AASHO BOND STRESS
$(0.75 \times 0.1 f'c \lesseqgtr 0.75 \times 350 \, psi)$

Table 2 this ratio is identified as $0.5u/u_{AASHO}$. However, at larger spacings a trend toward normal ratios exists. A somewhat crude but practical overall analysis will first be presented before presenting in Part B a more theoretical treatment which still lacks some validation.

Modification of AASHO Specification for Splices

A straight line multiplier to be applied to the allowable AASHO bond stress appears useful in designing a better splice. The data of Fig. 4 lead to an average ratio:

$$0.03 + 0.158 \ S/D$$

If this is dropped by 0.08 (roughly one standard deviation) it becomes:

$$0.158 \ S/D - 0.05$$

This relation could be used directly with the AASHO bond stress for design if one would accept a brittle failure mode at the first yield of the reinforcing. However, good design means the avoidance of a brittle failure wherever possible, which is probably best specified by lowering the permissible bond stress to 80 percent of the above, leading to a multiplier of

$$0.13 \ S/D - 0.04$$

While this multiplier is less than 1 until S/D becomes 8, it should be noted that present data stop at S/D of 6 and are based on using 2 in. of clear cover. For practical spacings of retaining wall splices the AASHO specification for #11 bars is less safe than desirable and for very close spacings it is barely safe at service loads.

Alternatively, and to obtain the same end result, the splice length as currently specified by AASHO might be divided by this "multiplier" to give the following for #11 bars, with an absolute minimum of 19D for large spacings:

For f_y = 40 ksi and f_c' = 3500 psi, L_s = 19D $\div$ (0.13 S/D - 0.04)

S/D	S	Reqd. L_s	Now Specified (for all size bars and spacings)
3	4.2"	54D	19D
4	5.6	40D	19D
5	7.0	31D	19D
6	8.5	26D	19D
8 or over	11.2 or over	19D	19D

For f_y = 60 ksi and f_c' = 3500 psi, 1.5 times the above lengths are required.

These relations have been verified only for #11 bars, but four samples with #8 bars indicate the same bond stress multiplier would be appropriate.

General Comments

By design these members were tested to give the necessary L_s values for retaining walls. For constant moment splices, with equal stresses at each end, more length is needed, probably 15 to 25 percent. The data are compared with a semitheoretical analysis in Part B and the results there look promising for more general use when better verified.

A few special cases of interest are shown on Fig. 5. The "x" marks indicate that either a single splice (one bar continuous, in beams #19, #28, and #3a) or a staggered splice (one starting where the other is complete, beam #20) is usually more effective, by 25 percent or more.

In the single specimen where #11 dowels were spliced to #9 main bars (beam #23, marked by a triangle) the unit stresses in the #9 and #11 bars were about the same. The strength was roughly 10 percent lower, which is within the expected scatter range.

A curved beam face (beam #25), representative of a part of a circular pier, including ties typical in such a case, showed particularly well when evaluated on the basis of the most highly stressed splice (the one farthest from the compression face).

The theory developed in Part B indicates that a lower stress at one end of the splice is advantageous, but heavy shearing stresses may offset this when the one stress is _very_ low.

At large S/D ratios a detailed study shows that the efficiency of a splice drops some with the increasing length, but this influence is less than the influence of S/D. Data are not adequate to clarify this point.

Where U-stirrups are feasible, the tests indicate a possible 40 to 100 percent gain in stress transfer, although probably this device is not practical for walls. Only a few such tests were made.

FIG. 5 BOND EFFICIENCY IN TERMS OF AASHO.
SPECIAL CASES MARKED WITH ARROWS.

Relationship to ACI Code Requirements

The data have been analyzed again in Fig. 6 in terms of the ACI Code provisions for splices. Ignoring single splices and splices with stirrups, the logic used in connection with Fig. 4 leads to a bond multiplier of

$$0.25 \ S/D - 0.14$$

which becomes unity at S/D of 4.6. Although this multiplier indicates the ACI Code is much closer to the test data than the AASHO specification, it is noted that this correction leads to splice lengths for #11 bars some 15 percent greater than the corrected AASHO values. For f_y = 40 ksi and f_c' = 3500 psi:

$$L_s = 28.4D^2/(0.25 \ S/D - 0.14)$$

S/D	S	L_s	For #11	Code for #11, Spacing Closer than S/D = 12
3	4.2"	$46.7D^2$	66D	40.2D
4	5.6	$33.0D^2$	47D	40.2D
5	7.0	$25.6D^2$	36D	40.2D
6	8.5	$21.0D^2$	30D	40.2D
8	11.2	$15.3D^2$	22D	40.2D

For f_y = 60 ksi and f_c' = 3500, 1.5 times these lengths are required.

The 15 percent differential appears partially due to greater scatter when these data are related to $\sqrt{f_c'}$ and partially to a slight unintended slant to the data caused by a concrete strength f_c' greater than 3500 psi in roughly 50 percent of the specimens. This raises the bond ratios under the AASHO specification which limits the basic allowable bond to 350 psi for f_c' of 3500 psi or more.

For #8 bars (4 specimens) the data plot unfavorably low and suggest that L_s as a multiplier of D might have to be increased as much as 30 percent above that for the #11 bars. It happens that if the equation above (in terms of D^2 and S/D) is multiplied by a 1.3 factor, the L_s values required for the #8 bars are nearly the same as the corrected AASHO values. However, four samples are not enough to justify the recommendation of a specific correction factor under this code.
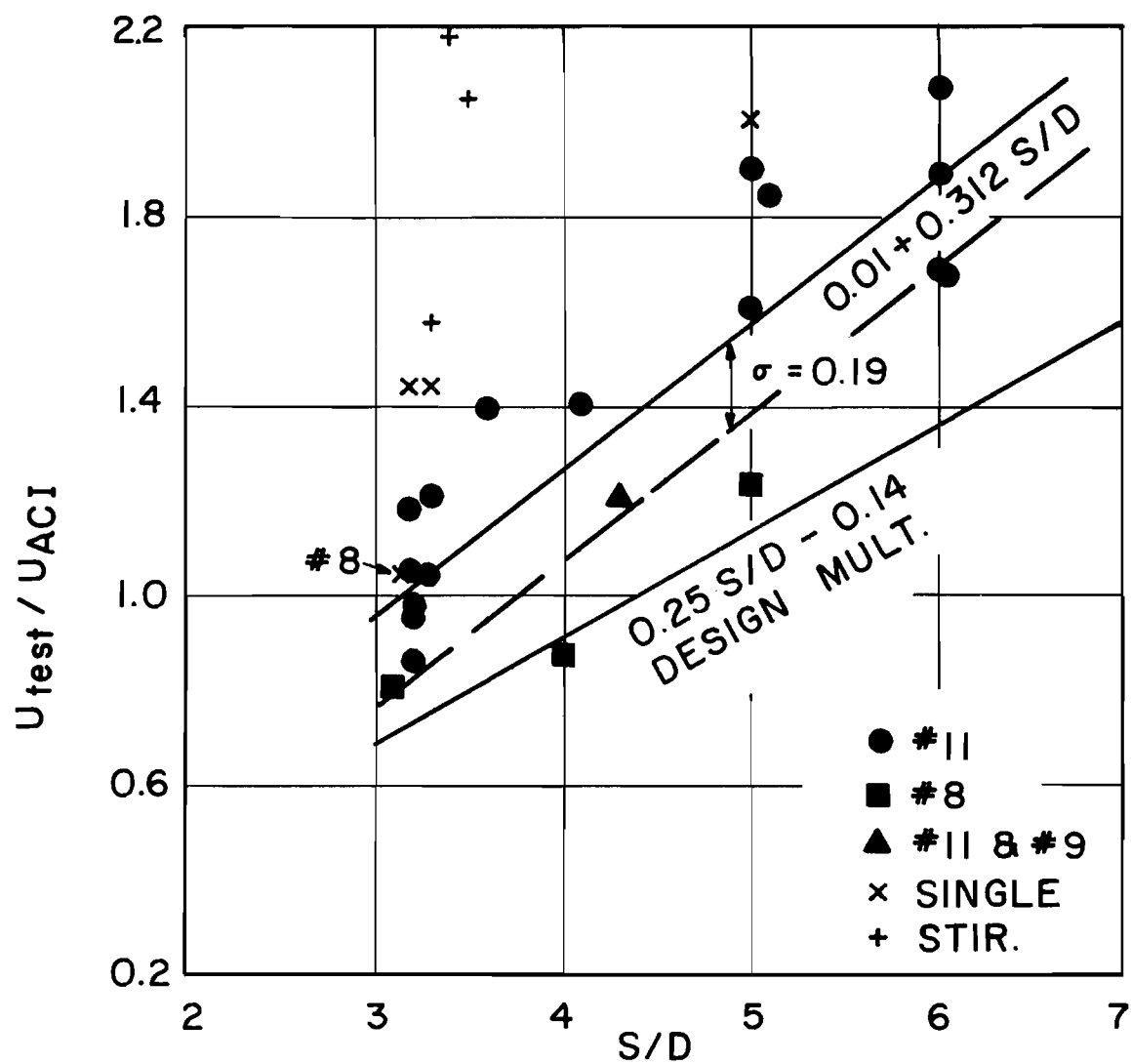
FIG. 6 BOND EFFICIENCY IN TERMS OF ACI
CODE BOND STRESS
$(9.5\sqrt{f_c^!}/D)(0.75/1.2)$ psi

Conclusions and Recommendations

In retaining wall splices at ordinary spacings, the AASHO specification (1965, 9th Edition) is shown not to be a safe guide unless seriously modified.

Based on the use of 2 in. clear cover over the bars, f_y = 40 ksi and f_c' = 3500 psi, the recommended lap splice length is increased to

$$L_s = 19D \div (0.13 \ S/D - 0.04) \gneq 19D$$

which has been verified for S/D up to 6 for #11 bars and also seems to fit #8 bars. Consistent with the AASHO specification, the value of L_s must increase linearly with f_y and with the ratio $3500/f_c'$, the latter only where f_c' is _less_ than 3500 psi.

On the basis of only 4 specimens, staggering of splices or the splicing of only half the bars at a given cross section would permit splice length L_s to be reduced to 80 percent of the above.

These recommendations do not apply for splices in a constant moment region, which should be longer as noted in Part B. Nor do they apply for less than a 2 in. clear cover, although Fig. 12 (Part B) suggests very tentatively that C/D = 1 might mean minimum splice lengths of 36D.

PART   B

A THEORY FOR SPLICES

Radial stresses around deformed bars wherever bar stress is changing have long been assumed. Recently Professor Goto in Japan has shown experimentally that at high steel stresses a tension bar embedded in a prism of concrete will not only develop transverse cracks in the prism but also internal cracks radiating from each transverse lug. These cracks are not perpendicular to the bar but in effect develop a truncated hollow cone of concrete bearing against the lug. These essentially parallel conical shells develop the change in bar tension by inclined compressive forces which are separated by the inclined cracks. This seems to be the manner by which tangential splitting stresses are developed near ultimate.

The following analysis makes the simplest possible basic assumption, that the radial and longitudinal stress components in the concrete are equal.* Calculations made on this basis coordinate well with split cylinder test strengths.

The second assumption is based on test data from the strain gage readings for this series of tests. As documented below, in spite of very different initial and intermediate distributions, <u>at ultimate</u> the variation in steel stress along the splice is essentially linear from zero at one end to maximum at the other; and this holds in both directions even when stress at one end is much lower than at the other.

Close examination of the failed specimens indicated two splitting failure patterns and pointed toward a third for thinner cover or wider spacing than used in this investigation:

1. At close spacings a crack along the plane of the bars which often went so far as to split off the entire cover over the splice; designated here as a side split failure.
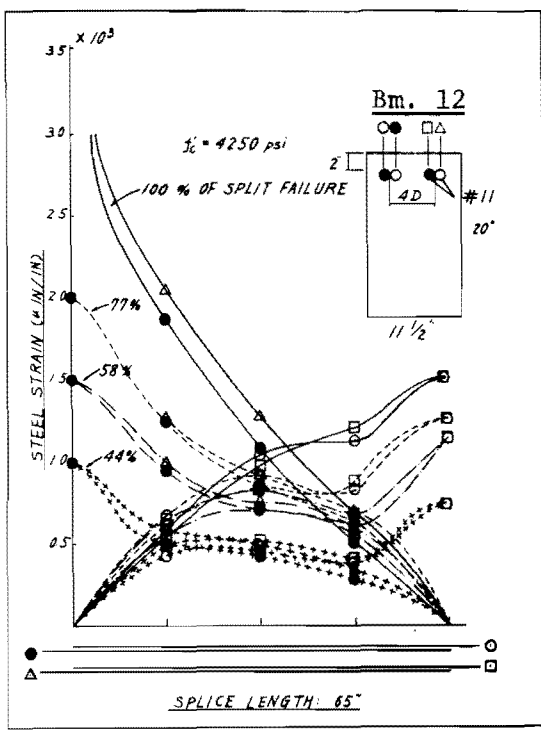
---

*Photographs made by Professor Goto would indicate an angle of possibly 50 or 55 degrees, which would mean even a larger splitting component.

2. Similar to the side split failure, except that there first developed longitudinal cracks on the tension face over the splices and the side split developed later to bring about failure; designated here as a face-and-side split failure.

3. Where cover is thin or lateral splice spacing wide, the initial tension face crack may be followed by the forcing out of a V-wedge of concrete over the bar. No such failure occurred in this investigation, but it shows on some earlier bond test pictures. This failure is designated as a V-type failure.

Bar Stress Along Splice

Resistance strain gages placed at the quarter points of splices indicated the general stress distribution along the splice. Although some variation showed between specimens, Fig. 7a is a typical strain record, simplified by showing data at only four load levels. The final strains can be interpreted as the stresses shown in Fig. 7b. Although the final stresses do not produce precisely straight lines (and might vary even more if gages were closely spaced over the 65-in. splice length), it is judged reasonable in the present state of the art to consider them straight. The slight curve at the upper left is probably the result of excessive splitting at the higher stressed end. The authors are inclined to revise their earlier ideas of splitting as a totally bad phenomenon to a concept of splitting as a device which accommodates the excessive steel strains in such a way as to develop a near optimum resistance in the concrete over a long length. A shorter 33 in. splice at 94 percent of ultimate is shown in Fig. 7c, and a longer splice with (arbitrary) minimum stirrups in Fig. 7d. The dashed lines marked "ACI" show the change in stress which the ACI Code assumes will take place. At the wider spacings the ACI Code is conservative.
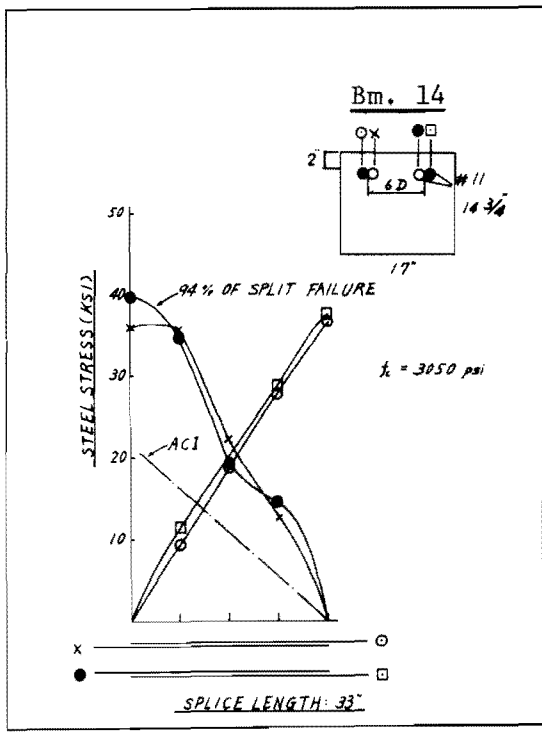
Some other failure conditions are shown in Fig. 8. With one bar continuous (unspliced) in Fig. 8a, the spliced bar takes less than 50 percent of the total tension at the ends of the splice and more than 50 percent at midlength. A flexural failure pattern for 4 splices is shown in Fig. 8b, a diagonal tension failure in Fig. 8c, and a splitting failure in a curved top beam in which the center bar took more than its share in Fig. 8d.
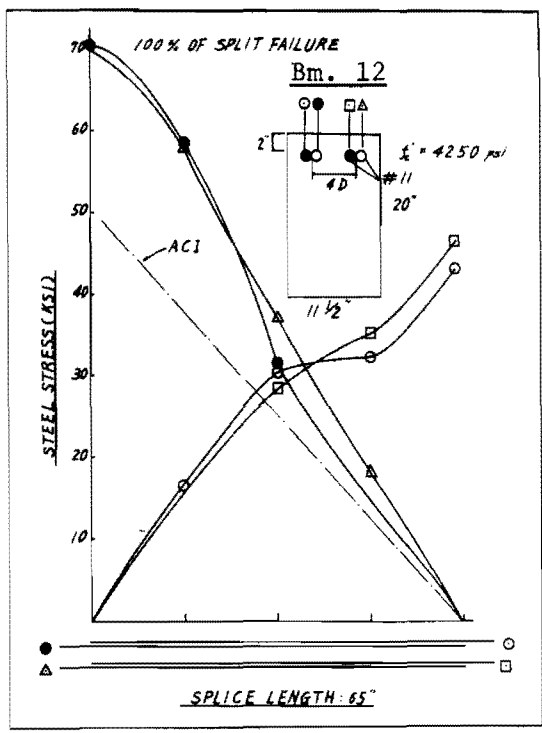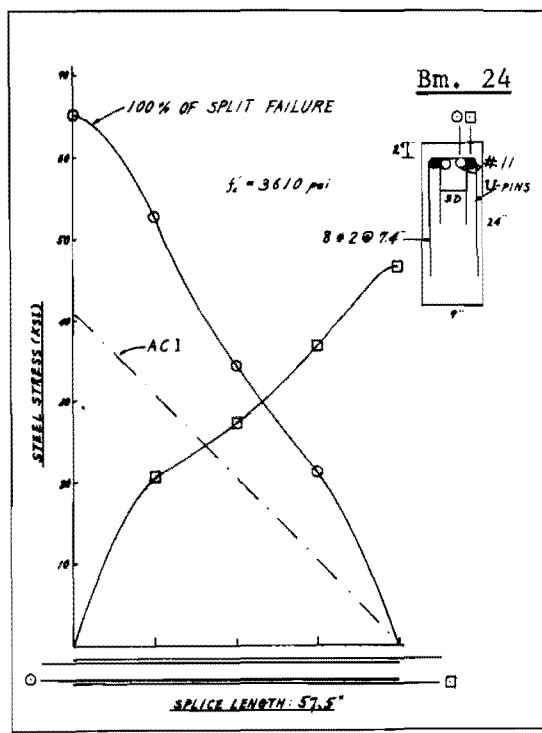
Fig. 7. Stress distribution along splice. Note that the last data
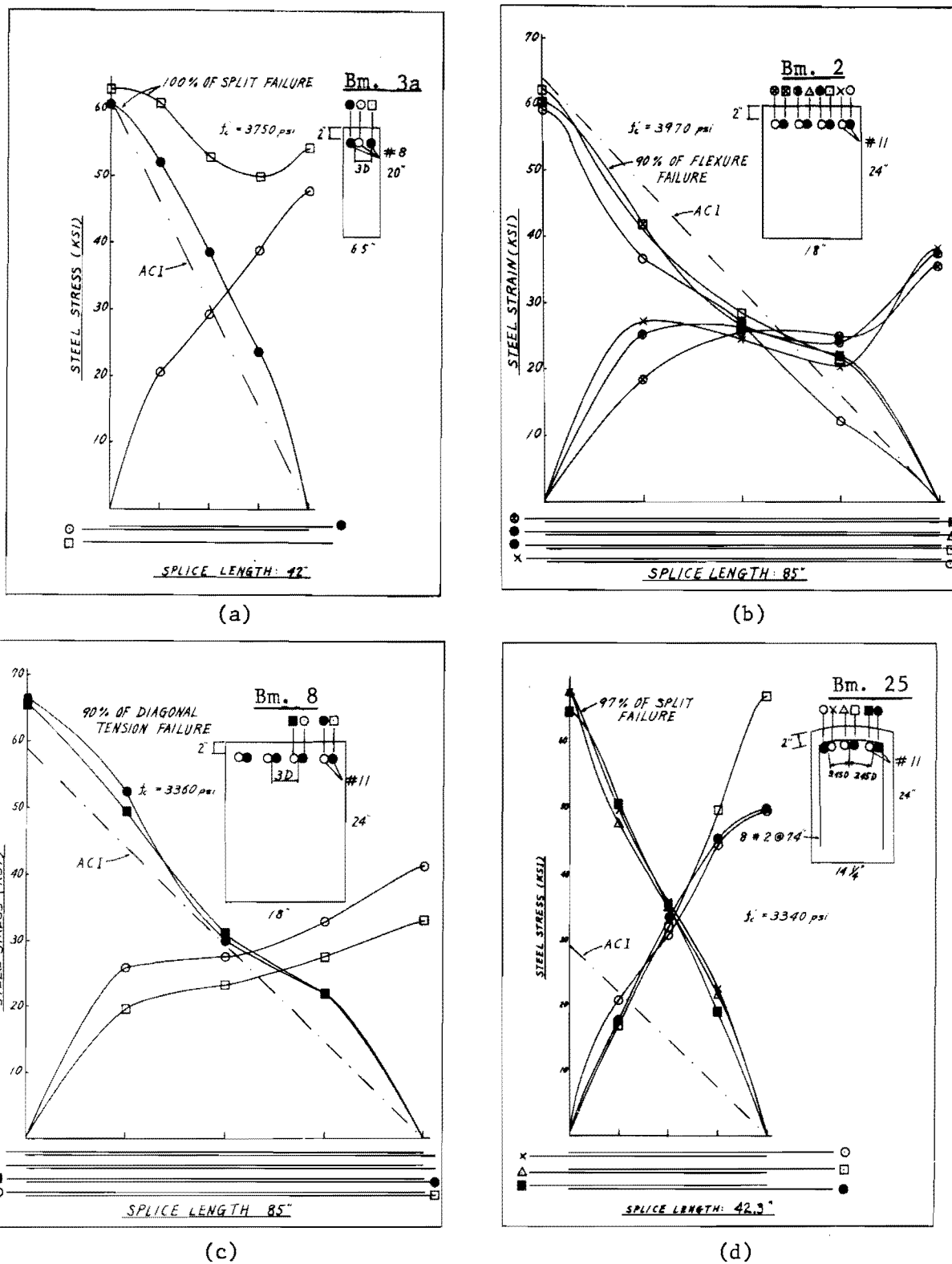in (c) are at 94% of ultimate.

Fig. 8. Stress distribution along splices for special cases. (a) One
bar unspliced. (b) Nonlinear; flexural failure with data at
90% of ultimate. (c) Some nonlinearity; diagonal tension
failure with data at 90% ultimate. (d) Curved face beam.

In some beams gage problems gave less complete records and there were variations not shown in Figs. 7 and 8, but the general pattern seems well-established. The following analyses assume bar stresses linear from zero to the measured strain (stress) at the other end of the splice.

Side Split Failure

Although the edge splitting sometimes evidenced the presence of shear by a somewhat flat saw-tooth outline, the final failure plane was essentially a horizontal one (in the plane of the bars). For analysis the unit radial force at the bar was arbitrarily assumed equal to the unit bond force on the bar surface. Then in Fig. 9, on the higher stressed bar

$$u = \frac{A_s f_{su}}{\pi D L_s} = \frac{D f_{su}}{4 L_s} = \text{radial unit force}$$

This leads to a splitting force on the diameter of bar, per unit length,

$$= uD = D^2 f_{su}/4L_s$$

On the other bar, similarly, the splitting force per unit length is $kD^2 f_{su}/4L_s$, for a total splitting force on __two__ splices of $2(1 + k)D^2 f_{su}/4L_s = (1 + k)D^2 f_{su}/2L_s$ per inch of length. The concrete area resisting splitting is b - 4D or 2S - 4D for a unit length which gives an average splitting stress on the concrete

$$f'_t = \frac{(1 + k)D^2 f_{su}/2L_s}{2S - 4D} = \frac{(1 + k)f_{su}D}{4(S/D - 2)L_s} \tag{1}$$

Based on the observed k and f_{su}, the calculated value of f'_t is tabulated in Table 2 and the next column shows the ratio of this value to the split cylinder value of f'_t. (For the face-and-side split failures a different relation, developed below, is necessary to calculate f'_t.) The ratio was low where failure in flexure occurred and high where stirrups existed (because the ratio at this time ignores stirrups). The diagonal tension failures also indicate by their ratios that splitting was close to its limit.

FIG. 9. SPLITTING FORCES FOR SIDE SPLIT FAILURE
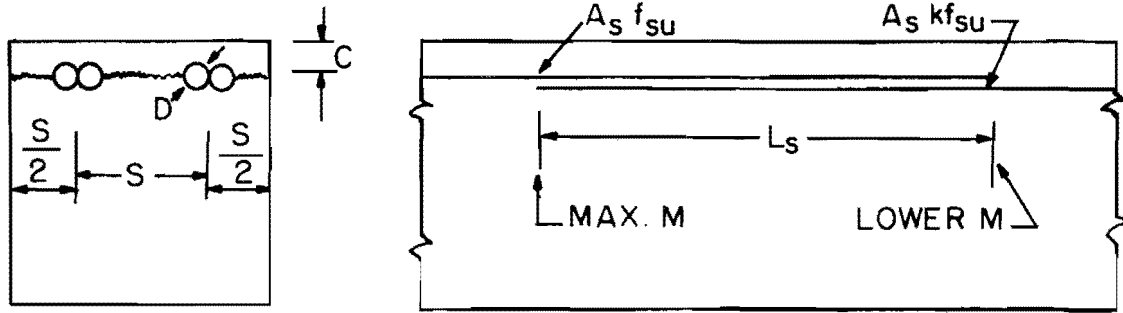
$$\frac{k f_s A_s}{\pi L_s} \quad \frac{f_s A_s}{\pi L_s} \quad \frac{k f_s A_s}{\pi L_s} = \frac{k D^2 f_{su}}{4 L_s}$$

$$\frac{k f_s A_s}{\pi L_s} \qquad \frac{f_s A_s}{\pi L_s} \qquad \frac{f_s A_s}{\pi L_s} \qquad \frac{k f_s A_s}{\pi L_s}$$
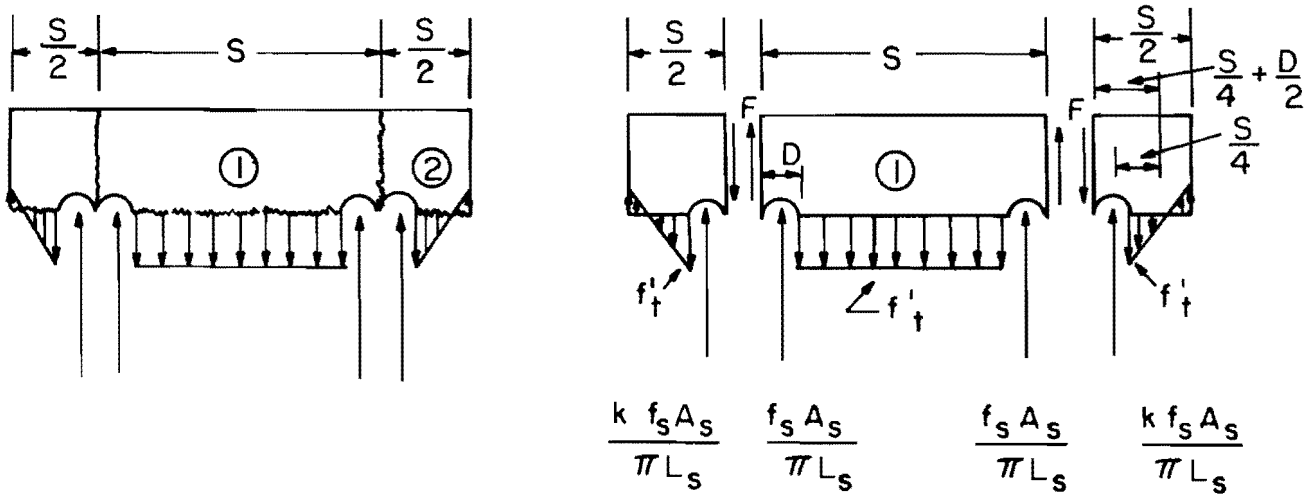
FIG. 10. FACE - AND - SIDE SPLIT FAILURE
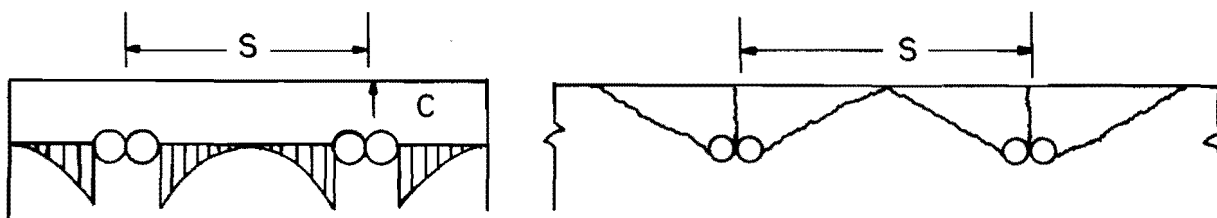
FIG. 11. V – TYPE FAILURE WHERE C/S IS VERY SMALL

Face-and-Side Split Failure

The final failure in the face-and-side split case was almost the same as in the side split case. Although the first edge cracking tended to be a little farther from the tension face, the final failure showed less difference. The analysis assumes splitting forces as before and lengthwise cracks existing on the tension face over the splices which prevent transverse forces perpendicular to the crack but which (by aggregate interlock) transmit substantial shears. The schematic arrangement of forces on a transverse section is shown in Fig. 10, along with sketches of the separate pieces at failure. Symmetry laterally leaves two free bodies to consider. On the center free body, summation of vertical forces leads to

$$\frac{2f_s A_s}{\pi L_s} + 2F = f_t'(S - 2D) = 0$$

$$F = \frac{1}{2} f_t'(S - 2D) - \frac{f_s A_s}{\pi L_s} \tag{2}$$

With the corner free body, if one makes the oversimplifying assumption that the resulting stresses can be based on $P/A + Mc/I$, the limiting stress is

$$f_t' = \frac{(-F + kf_s A_s/\pi L_s)}{(0.5S - D)} + \frac{[(kf_s A_s/\pi L_s)0.25S - F(0.25S + 0.5D)]}{(0.5S - D)^2/6}$$

If the value of F from Eq. 2 is inserted, the equation can be rearranged* to

$$f_t' = \frac{f_s \pi D^2}{4\pi L_s}\left[\frac{2(1 + k)S + (2 - k)D}{(2.5S + D)(0.5S - D)}\right] = \frac{f_s D}{L_s}\left[\frac{2(1 + k)S/D + (2 - k)}{(5S/D + 2)(S/D - 1)}\right] \tag{3}$$

When a given spacing S is expressed as a multiple of D, or D as a fraction of S, Eq. 1 and 3 reduce to the forms:

$$f_t' = (f_s D/L_s) \times \text{constant}, \quad \text{or} \quad f_s = (f_t'L_s/D) \times \text{constant} \tag{4}$$

For Eq. 4 the constant for a given spacing S is such as to lead to a lower f_s than that given in Eq. 1 for the side split case, that is, the corner free bodies are less efficient than in the side split case.

---

*With experience this equation can probably be simplified. It is overly complex for the assumed accuracy.

As either of the above failure patterns is considered with wider and wider spacings, or thinner cover C, it becomes less probable that a uniform f_t' will exist between the splices. At some spacing for each cover the stress midway between the two splices probably drops to zero and a separate flat V-type failure over each single splice becomes probable, as sketched in Fig. 11. No such failures occurred in this investigation but an earlier test showed this failure which forms an upper limit on the possible value of either Eq. 1 or 4. It appears that the ultimate f_{su} should then vary linearly with the cover C, for splice length and other conditions the same.

Comparison of Test Results with This Theory

Although the above relations are undoubtedly oversimplified, essentially all the test results seem to agree with them within ± 15 percent. As mentioned earlier, Eqs. 1 or 3, as applicable, was solved for the splitting stress f_t' and these values are compared in Table 2 to the split cylinder strengths. A number of special cases--single splices with one bar continuous, unequal bars spliced, edge distance less than S/2--were calculated by minor variations of the above procedures. The final ratios of $f_{t(calc)}'/f_{t(cyl)}'$ in Table 2 are quite reasonable. With stirrups the computed f_t' is overly large, as it should be since this approach (to this time) does not include the strength added by the stirrups.

Wall Splices Versus Beam Splices

The first tests in the present series were studies of whether four splices at the same section, as in a wall of some width, were different in behavior from a narrower beam with two splices having the same center-to-center spacing. Unfortunately, these splices were at a close spacing which gave side split failures and showed no significant differential in their data. The later analysis of the face-and-side split cases seems inconsistent with probable strains in a wall, since the face-and-side split failure requires some lateral movement of the beam corner segments. In a continuous wall the face cracks can form, but it is difficult to visualize significant additional lateral movement.

Tentatively it is assumed (but still unproven) that in a wall, as wider spacings of splices are considered, the assumed uniform tension across the splitting section must become less uniform, making the resistance less efficient, that is, stronger but not stronger in full proportion to the width increase. At some wide spacing the flat V-type failure will govern and the possibility of the beam-type failure by a face-and-side split will be completely bypassed. This spacing limit should be sharply dependent on the face cover over the bars. If this hypothesis is correct, wall splices at spacings greater than 4D or 5D will be stronger than the corner splices in a beam which have the same splice spacing (laterally), that is, stronger than the test values reported here for $S/D = 6$.

Influence of a Variable Moment over Splice Length

All these tests had loadings which created a lower bar tension at one end of the splice than at the other. The theory developed above considers splitting as the result of <u>both</u> bar tensions, one bar at $A_s f_{su}$ and the other at $kA_s f_{su}$, where k is a factor less than unity. This results in the term $1 + k$ in both Eq. 1 and Eq. 3, and in the latter a second term, $2 - k$, small enough to be neglected. With this approximation the total splitting force is proportional to $1 + k$.* This implies that a splice in a constant moment zone must care for more splitting and should be designed for $2f_{su}$ instead of $(1 + k)f_{su}$. With $k = 1$ in Eqs. 1 and 3, these relationships seem applicable for splices in a constant moment zone:

Side split:
$$f'_t = \frac{2f_s D}{4(S/D - 2)L_s} = \frac{f_s D}{2(S/D - 2)L_s} \qquad (5)$$

Face-and-side split:
$$f'_t = \frac{f_s D}{L_s}\left[\frac{4S/D + 1}{(5S/D + 2)(S/D - 2)}\right] \qquad (6)$$

Design Chart

For any given k value, design-type charts can now be prepared schematically, although certain transition areas are still not clarified.

---

*Checks on test data indicate that $k = 0$ gives f_{su} values too high for an ordinary development length, probably because larger shears accompany this case and combine with the splitting forces.

The chart in Fig. 12 for k = 1 is for a fixed concrete strength and relates the design ultimate steel stress to splice length and spacing. The data are weighted in such a manner that the expected ultimate splice strength will correspond to $1.25f_y$ when f_y is entered in the chart for f_{su}. The ordinate shows the dependable design ultimate stress in ksi developed for a splice length of one bar diameter. Then f_y divided by this number gives the needed splice length L_s. The present chart in Fig. 12 for k = 1 for a given f_t' (or possibly $\sqrt{f_c'}$) is weakest in the upper horizontal limits based on the V-type failure and in the possible transition phases which remain to be investigated. For the side split failure the inclined line is straight and for the face-and-side split essentially straight. If k < 1, the limits would be parallel lines with all f_{su} values higher, as shown dotted for k = 0.75.

The equation lines can be separately compared with the data of this investigation, as in Fig. 13. For the side split failures most of the data fall between S/D of 3.1 and 3.3 and show considerable scatter. One value at S/D of 3.6 fits well. A #8 bar specimen at S/D of 4 falls substantially below the equation value. For S/D of 4.1 the face-and-side split failure occurred.

Figure 13 shows an average line, a 10 percent reduction line to offset some of the scatter, and the 0.8 factor line to assure strength beyond the yield point, hopefully to $1.25f_y$. With this line the designer can design the splice for a nominal f_y and still maintain a ductile type of failure. This procedure leads to Eq. 7 and 8 from Eq. 5 and 6, by insertion of

$$f_t' = 375 \text{ psi } (0.375 \text{ ksi}), f_c' = 3500 \text{ psi, and } k = 1.$$

Side split:
$$f_s(D/L_s) = 0.8[0.75S/D - 1.5]0.9$$
$$= 0.54S/D - 1.08 \tag{7}$$

Face-and-side split:
$$f_s(D/L_s) = 0.8\left[0.375\,\frac{(5S/D + 2)(S/D - 2)}{(4S/D + 1)}\right]0.9$$
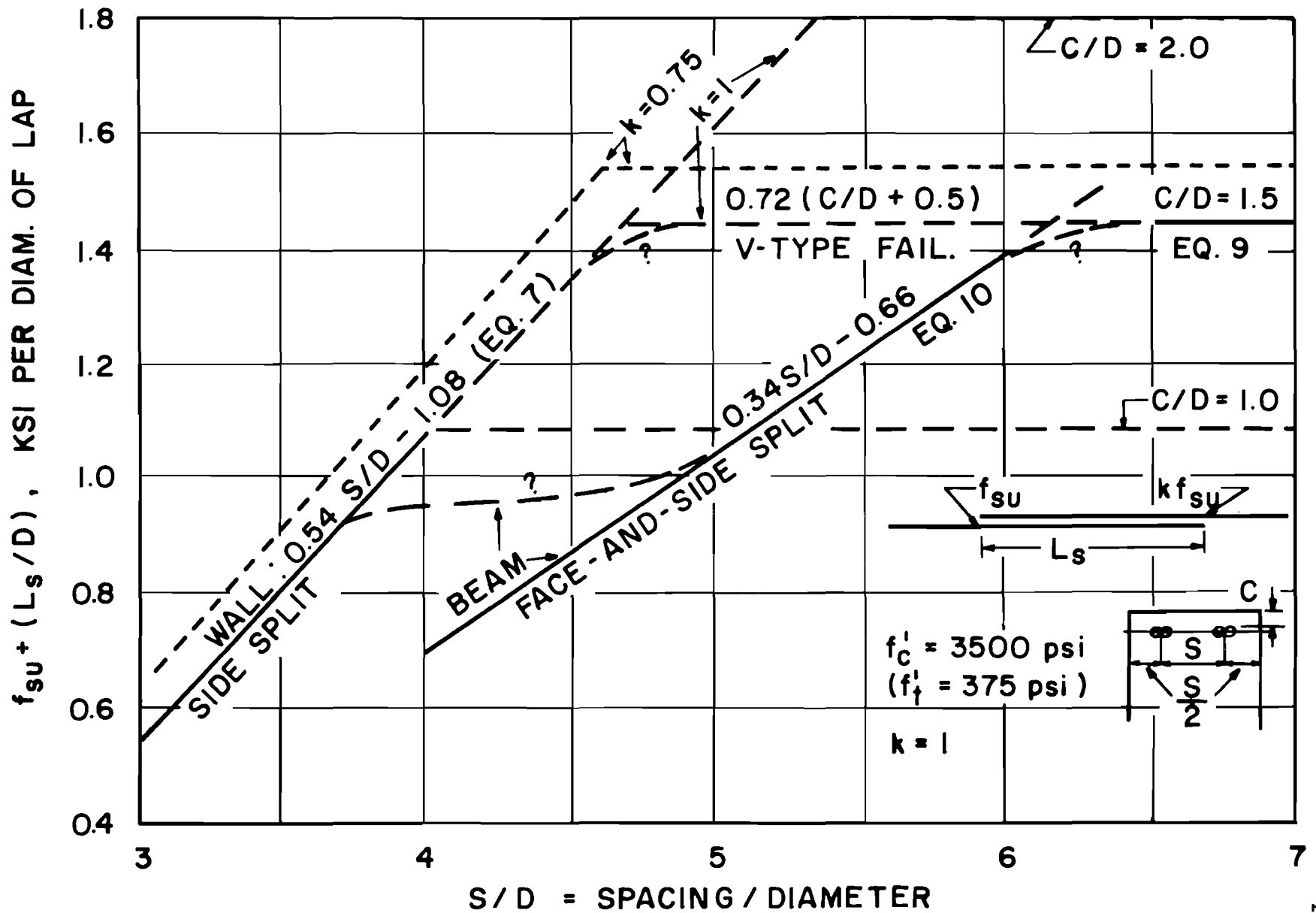$$= 0.270\,\frac{(5S/D + 2)(S/D - 2)}{(4S/D + 1)} \tag{8}$$
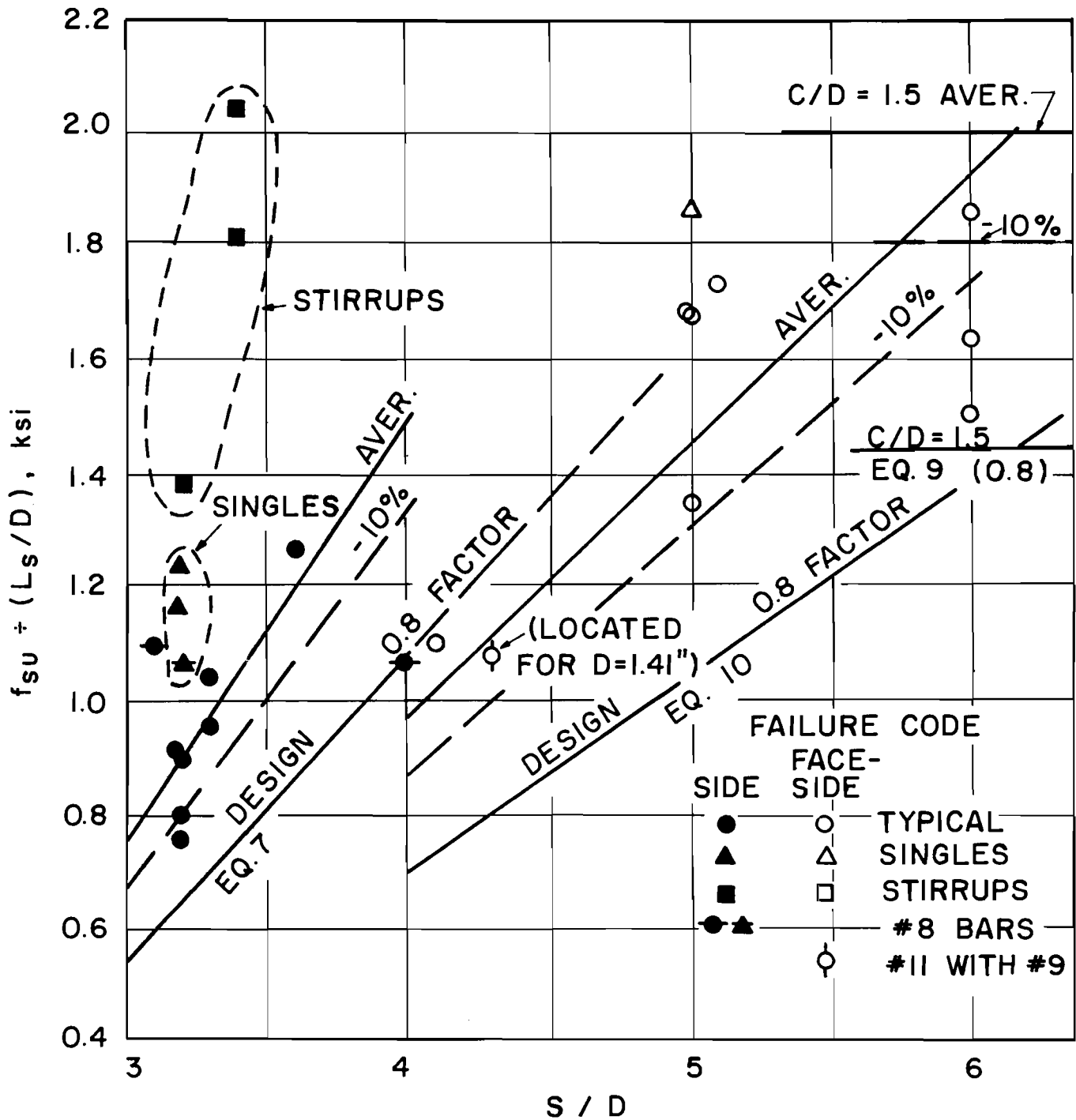
FIG. 12. SKELETON DESIGN TYPE CHART, TENTATIVE

FIG. 13 DESIGN EQUATION VS. TEST DATA

For the V-type failure the following equation is introduced as the best present guess for this condition, modified by factors as above:

V-type: $\quad\quad\quad\quad\quad f_s(D/L_s) = 0.8[0.375 \times 2.67(C/D + 0.5)]0.9$

$$= 0.72(C/D + 0.5) \quad\quad\quad\quad (9)$$

It also appears that in the useful range Eq. 8 for the face-and side split can be adequately and more simply expressed empirically as

Face-and-side split: $\quad f_s(D/L_s) = 0.34S/D - 0.66 \quad\quad\quad\quad (10)$

The horizontal limit lines representing V-type failures for various C/D ratios (where C is the clear cover) are based wholly on earlier data, reduced as in the other cases. These numerical values are very tentative. They would seem equally applicable as upper limits for either the side split or face-and-side split cases and appear particularly restrictive when cover is thin.

In at least certain cases, transition curves as sketched in Fig. 12 are still to be determined and probably will control. For instance, if C/D is large, it appears a wall splice will be defined at low S/D values by Eq. 7. As S/D becomes 6 or 7, it is almost certain that the resistance to splitting is not increased proportionately (compare Fig. 11) and the straight line of that equation probably curves (flattens) decidedly. For a beam with two splices, there must be a transition from Eq. 7 to Eq. 8 (or 10) and possibly another from the latter to Eq. 9.

A single empirical lower bound curve could be established for the whole range of S/D values covering all three equations. Such has not been developed because it was felt that the face-and-side split was probably not proper for wall splices and the separate curves look promising for further development. In the coming year these will be investigated further.

Conclusions

A tentative splitting theory for splices has been developed which seems to fit the test results with errors generally less than 15 percent. Transition zones between the three separate cases still need to be defined

and an assumed difference between wall and beam splices must be verified or disproved. Work is continuing in this direction.

Until this work is further advanced, detailed recommendations for design beyond those of Part A are not warranted.
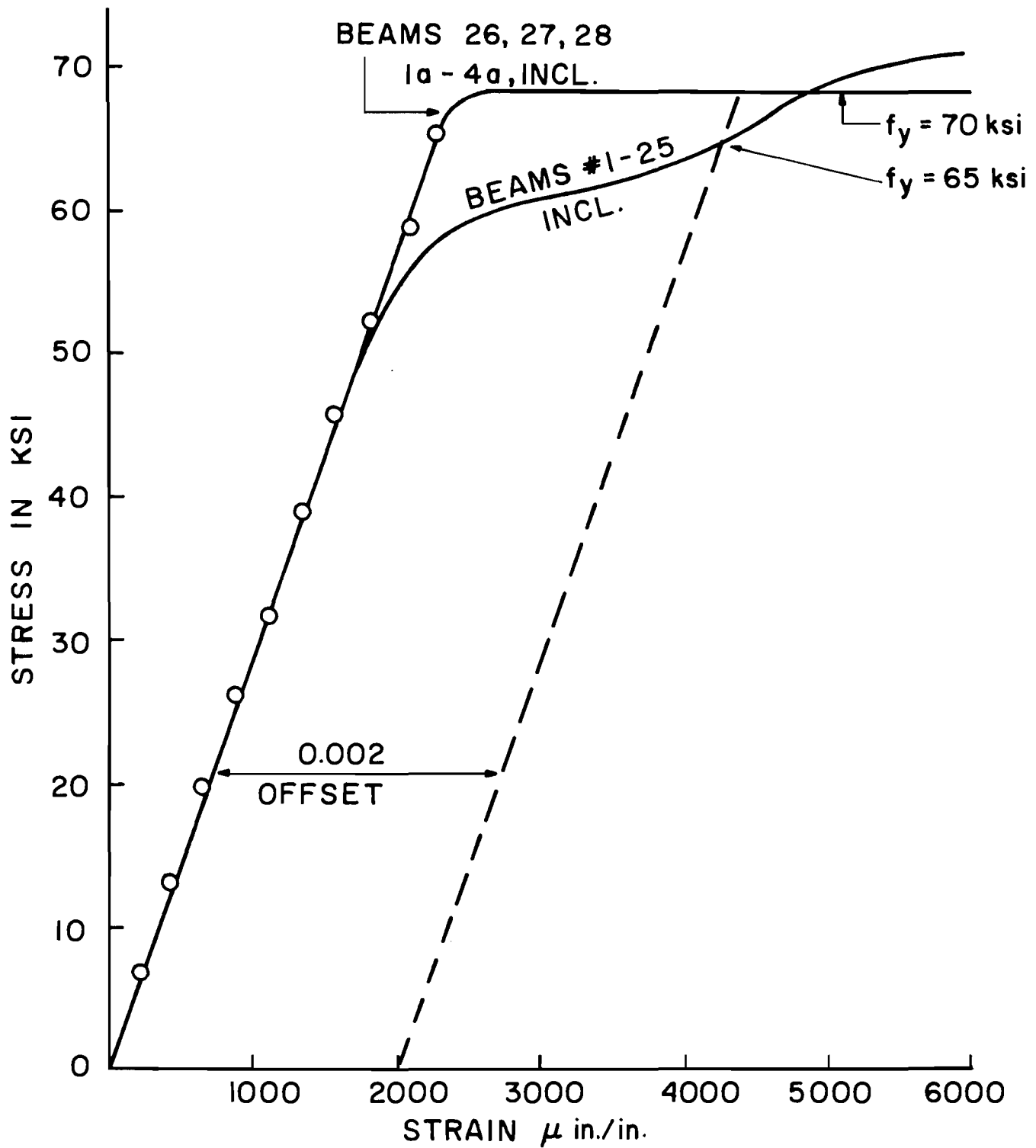
FIG. AI. STRESS-STRAIN CURVES FOR REINFORCEMENT